Supporting Information

Evaporation of drops containing silica nanoparticles of varying hydrophobicity: exploiting particle-particle interactions for additive-free tunable deposit morphology

Manos Anyfantakis,[1,2] Damien Baigl[1,2] and Bernard P. Binks[3]

[1]*École Normale Supérieure, PSL Research University, UPMC Univ Paris 06, CNRS, Department of Chemistry, PASTEUR, 24 rue Lhomond, 75005 Paris, France*

[2]*Sorbonne Universités, UPMC Univ Paris 06, ENS, CNRS, PASTEUR, 75005 Paris, France*

[3] *School of Mathematics and Physical Sciences, University of Hull, Hull, HU6 7RX, U.K.*

*Corresponding authors: E-mail: emmanouil.anyfantakis@ens.fr; damien.baigl@ens.fr; b.p.binks@hull.ac.uk

---

Contents

---

1) Text S1

The procedure followed for analysing the morphology of deposits emerging after sessile drop evaporation is described below; the relevant lengths used are depicted in Figure S8. First, we manually measured the lengths $l_{ring,L}$, $l_{ring,R}$ and l_{inter} covered by the left and the right and the deposit interior, respectively. Note that $D = l_{ring,L} + l_{ring,R} + l_{inter} = l_{ring} + l_{inter}$ denotes the diameter of the dry deposit. For cases where the ring lengths $l_{ring,L}$, $l_{ring,R}$ were ambiguous due the broadened ring shapes (*i.e.* for the drops containing 61% - 14% SiOH NPs), we employed calculated values using the average length of the left and the right rings, $\frac{l_{ring,L}(100\%)+l_{ring,R}(100\%)}{2} = \frac{l_{ring(100\%)}}{2}$, of the pattern corresponding to the most hydrophilic NPs (100% SiOH). Thus, the calculated ring lengths for another stain made of particles containing X% SiOH having a diameter $D_{(X\%)}$ were $\frac{l_{ring(100\%)}}{2D_{(100\%)}} D_{(X\%)}$. We further integrated the areas under the height profile curve for each ring, $a_{ring,L}$ and $a_{ring,R}$, as well as the interior, a_{inter}. We calculated the total ring length and area as $l_{ring} = l_{ring,L} + l_{ring,R}$ and $a_{ring} = a_{ring,L} + a_{ring,R}$, respectively. In the exceptional cases that one of the two rings was destroyed (e.g., during scanning), we assumed that $a_{ring,L} = a_{ring,R}$ and $l_{ring,L} = l_{ring,R}$. The next step was to divide a_{ring} and a_{inter} by l_{ring} and l_{inter}, respectively, to obtain the number density of deposited NPs per unit length. Finally, we divided the particle number densities with their sum and we obtained the normalized NP densities, A_{ring} and A_{inter}, as follows:

$$A_{ring} = \frac{\frac{a_{ring}}{l_{ring}}}{\frac{a_{ring}}{l_{ring}}+\frac{a_{inter}}{l_{inter}}} \quad \text{and } A_{inter} = \frac{\frac{a_{inter}}{l_{inter}}}{\frac{a_{ring}}{l_{ring}}+\frac{a_{inter}}{l_{inter}}} .$$

2) Text S2

To evaluate the extent of sedimentation and therefore its influence on the morphology of the deposits after drop evaporation, we calculate here the Péclet numbers corresponding to the three characteristic objects contained in our suspensions. The Péclet number is defined as $Pe = hU_{sed}/D$, where h is the initial drop height, U_{sed} is the sedimentation speed and D is the diffusion coefficient. We use drops of volume $V = 0.8$ µL, which display an initial contact angle $\theta \approx 65^{o}$. The drop base radius is typically $r \approx 0.9$ mm, which, assuming the drops adopt a spherical cap shape, corresponds to $h = r(1-\cos\theta)/\sin\theta \approx 0.6$ mm. According to the Stokes law, the sedimentation speed of a spherical particle (density ρ_p) falling in a fluid of dynamic viscosity η and density ρ_f is $U_{sed} = 2g(\rho_p - \rho_f)R_h^2/(9\eta)$, where g is the gravitational acceleration. Finally, assuming a spherical object, the diffusion coefficient can be calculated by the Stokes-Einstein-Sutherland equation: $D = k_B T/6\pi\eta R_h$, where k_B is the Boltzmann constant and T is the temperature (typically, in our experiments $T = 295$ K).

This calculation gives:

- $Pe \approx 0.007$ for *the primary particles* (for $R_h \approx 10$ nm)
- $Pe \approx 4.3$ *for the stable aggregates* (for $R_h \approx 85$ nm) and
- $Pe \approx 870$ for the few remaining *loose agglomerates* (arbitrarily using $R_h = 500$ nm)

Note that we here assume that the density of the object is always 2,200 kg/m^3 (this is the density of amorphous silica), which would hold for an object with homogeneous density (*i.e.*, for the primary particles). However, the stable aggregates, as well as the loosely packed agglomerates, should have a much lower density; as a result, the corresponding Peclet numbers presented above might be overestimated (*i.e.*, the effect of sedimentation is overestimated). Furthermore, we assumed a spherical shape (for calculating both the diffusion coefficient and the

sedimentation velocity). This assumption should hold for the stable aggregates (which should be the majority of objects in our samples), as indicated by the R_h/R_g ratio (= 1.2, see Stocco *et al*., *Soft Matter* **2009**, *5*, 2215), as well as for the primary particles (see Zang *et al*., *Phys. Chem. Chem. Phys.* **2009**, *11*, 9522).

3) Supplementary Figures S1-S10

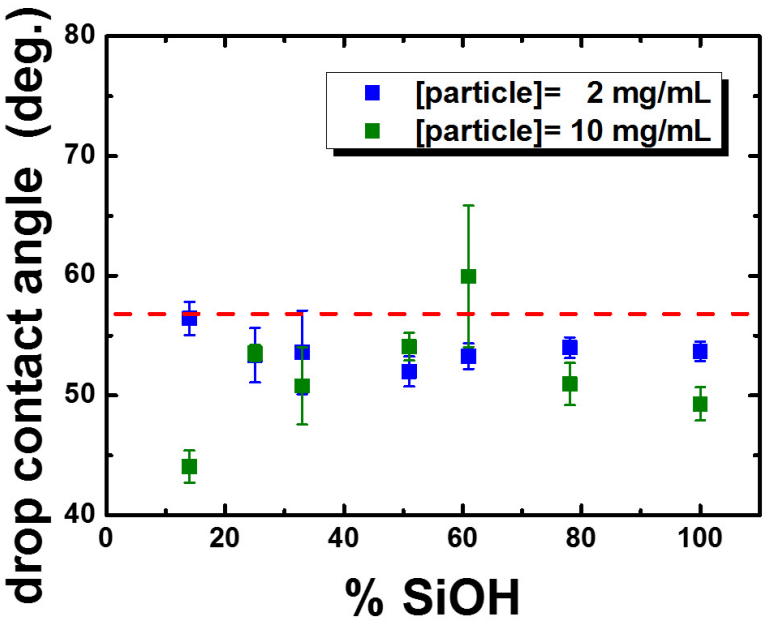

Figure S1. Contact angle of drops of aqueous silica particle dispersion in air on glass coverslips averaged in the time interval (70 - 80 s) as a function of the surface fraction of SiOH groups per particle, for two different particle concentrations. Symbols and error bars indicate mean ± std. dev. for at least 7 independent measurements. The dashed line indicates the contact angle of pure water on similar substrates (56.8 ± 4.7° on 16 independent measurements). Experiments were conducted at 22.1 ± 1 ºC.

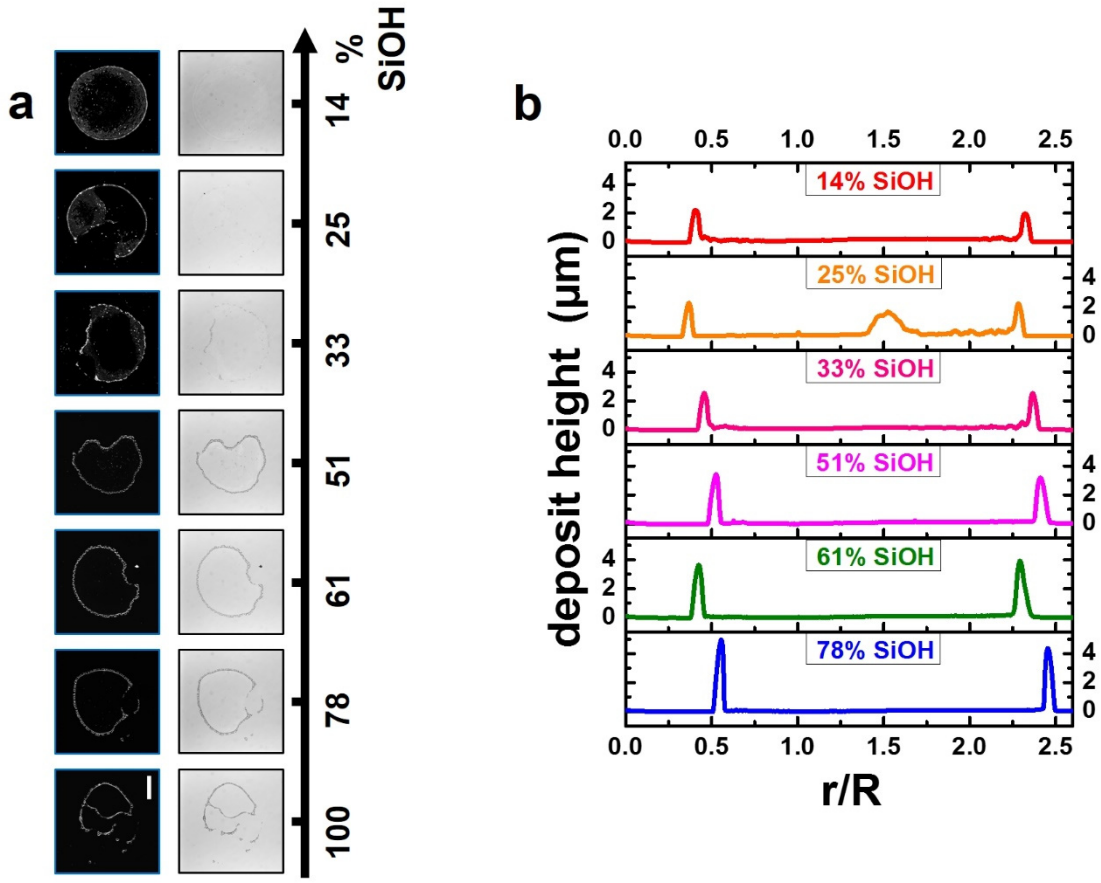

Figure S2. Morphologies of the patterns formed after the evaporation of sessile drops (0.8 µL) of the most dilute suspensions examined (0.5 mg/mL), deposited on glass coverslips. Suspensions contained silica nanoparticles possessing varying amounts of surface SiOH groups (100% - 14%) dispersed in water. (a) Transmission brightfield as well as darkfield microscope images of the dry deposits are shown. For clarity, the contrast of the darkfield images of the 33%, 25% and 14% SiOH nanoparticles was maximized using the ImageJ software. The scale bar is 500 µm. (b) Corresponding height profiles measured with a stylus profilometer. R is the deposit radius and r is the radial dimension. The height profile of the deposit resulting from the drying of the 100% SiOH suspension drop is not shown due to its highly irregular shape.

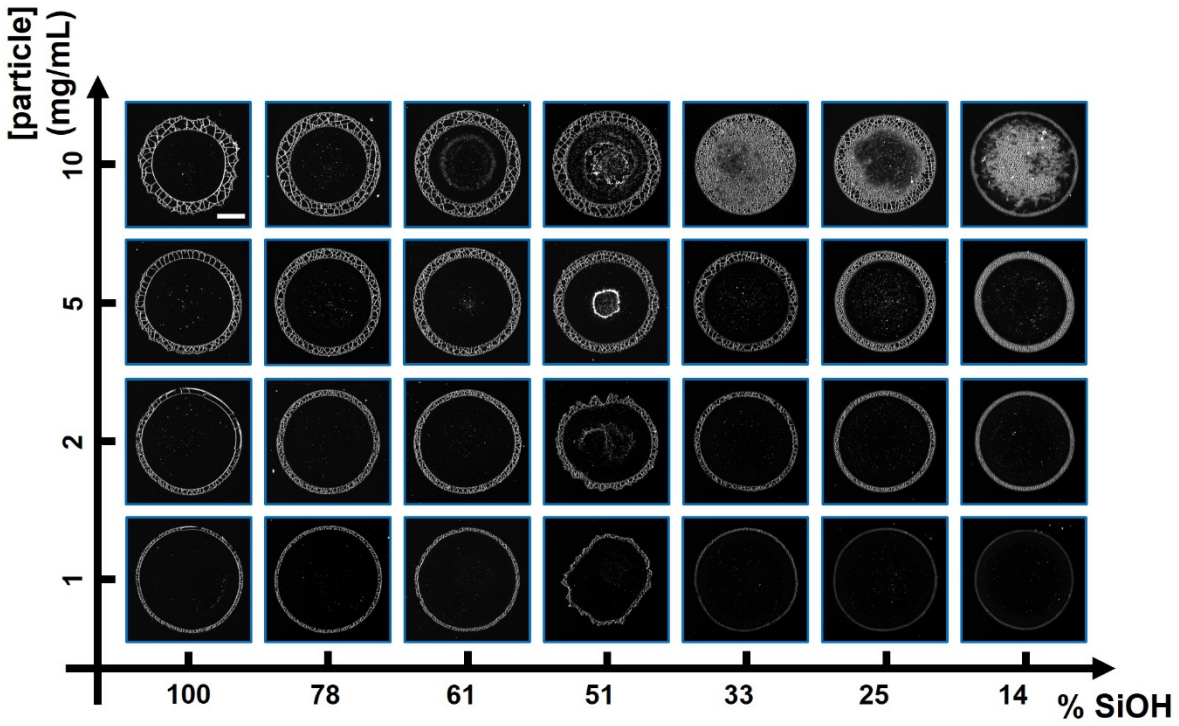

Figure S3. Transmitted darkfield microscope images of deposits obtained after the evaporation of sessile drops (0.8 μL) of silica nanoparticle suspensions deposited on glass coverslips. Suspensions containing nanoparticles with varying contents of surface SiOH groups for an extended range of particle concentrations (1-10 mg/mL) were examined. The scale bar (see top left image) is 500 μm.

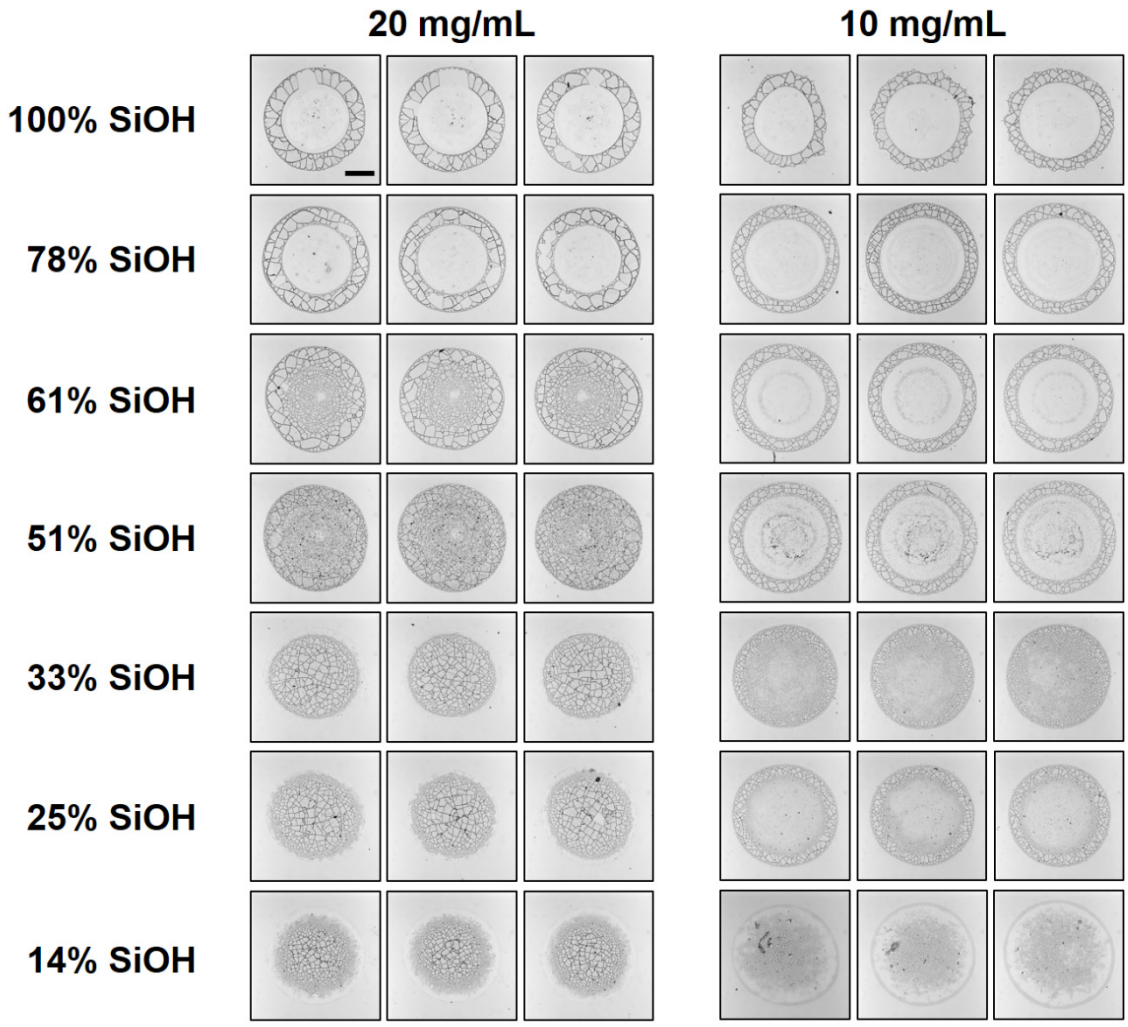

Figure S4. Transmission brightfield microscope images of deposits obtained after the evaporation of sessile drops (0.8 µL) of silica nanoparticle suspensions deposited on glass coverslips. Triplicates for two particle concentrations (20 mg/mL and 10 mg/mL) and varying contents of surface SiOH groups are shown. The scale bar is 500 µm.

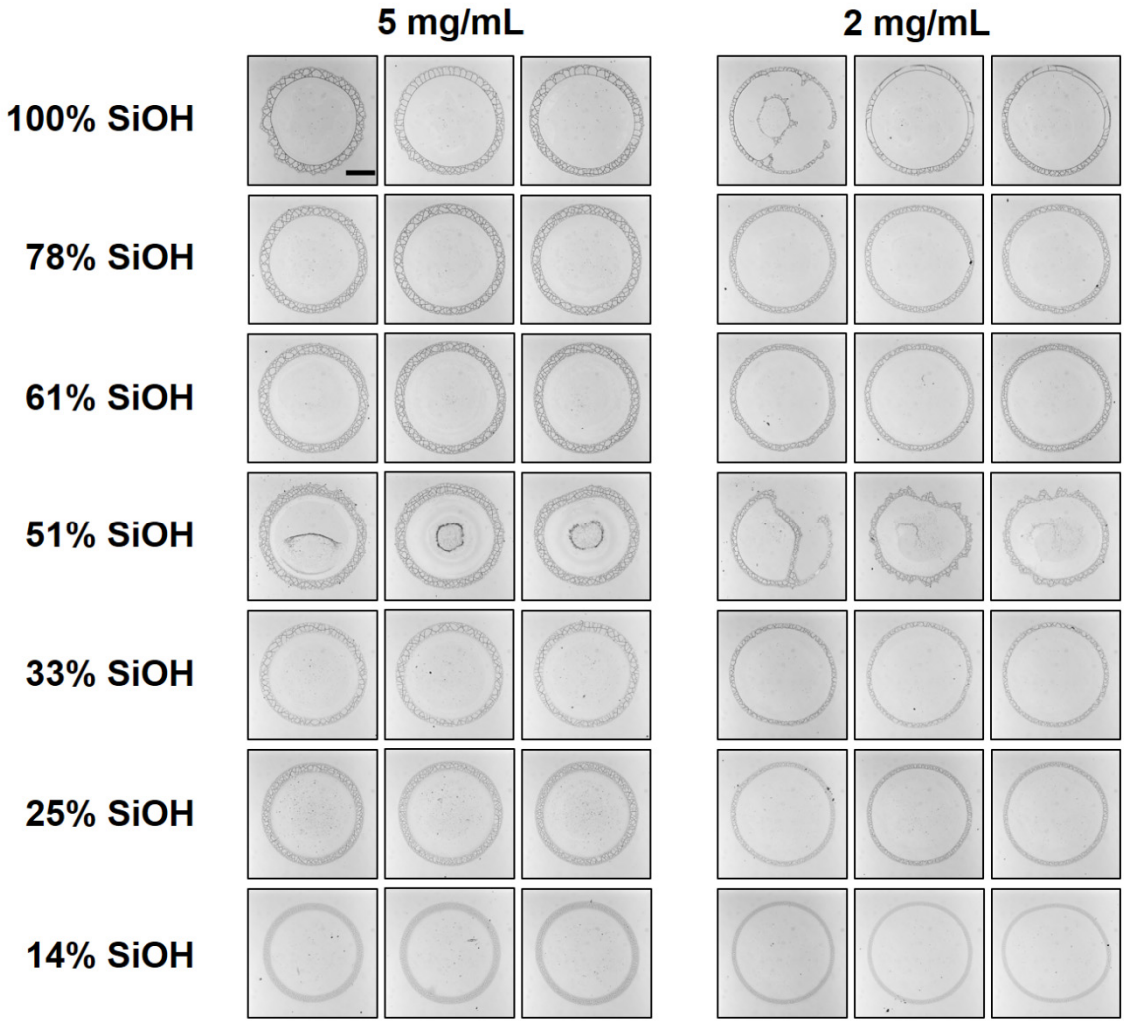

Figure S5. Transmission brightfield microscope images of deposits obtained after the evaporation of sessile drops (0.8 µL) of silica nanoparticle suspensions deposited on glass coverslips. Triplicates for two particle concentrations (5 mg/mL and 2 mg/mL) and varying contents of surface SiOH groups are shown. The scale bar is 500 µm.

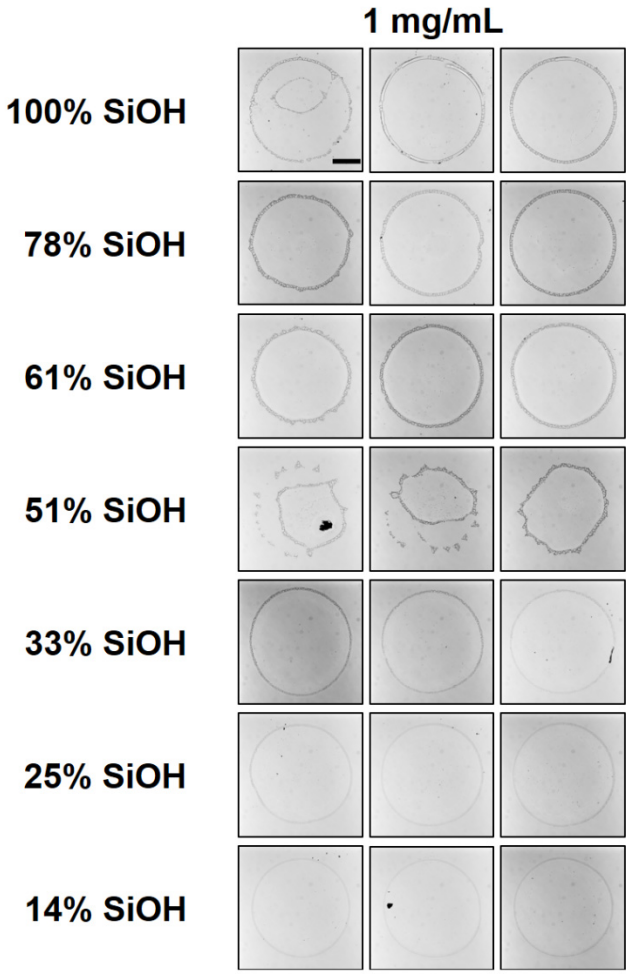

Figure S6. Transmission brightfield microscope images of deposits obtained after the evaporation of sessile drops (0.8 µL) of silica nanoparticle suspensions deposited on glass coverslips. Triplicates for one particle concentration (1 mg/mL) and varying contents of surface SiOH groups are shown. The scale bar is 500 µm.

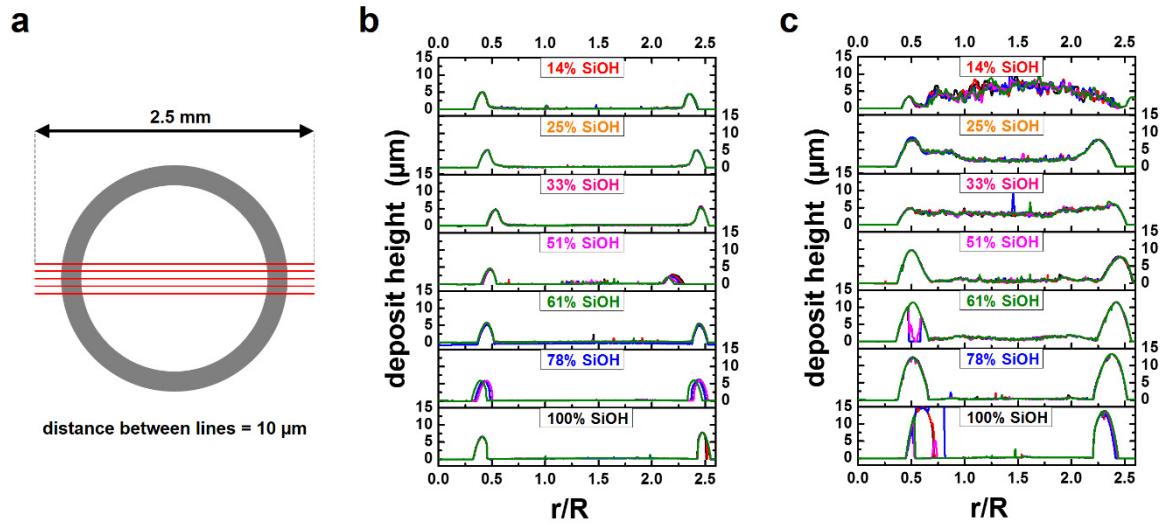

Figure S7. (a) Scheme of the 5 parallel profilometry scans performed along each deposit diameter. (b), (c) Height profiles according to the 5 individual scans performed for different SiOH contents at a particle concentration of (b) 2 mg/mL and (c) 10 mg/mL. There is one color per individual scan. Note that most of the scans are superimposed and cannot be distinguished from each other.

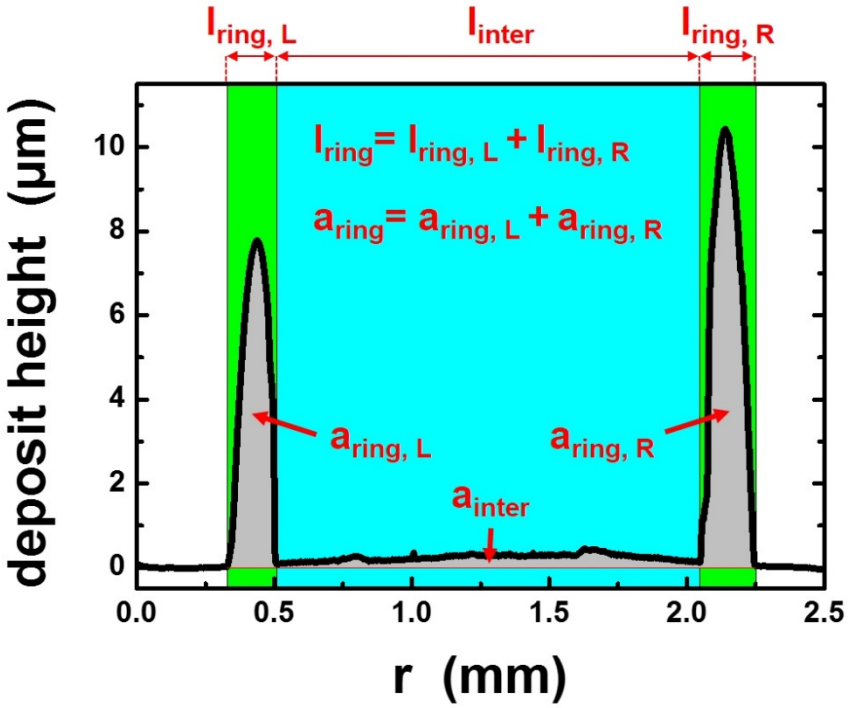

Figure S8. Schematic showing the relevant lengths (indicated with dashed lines) and integrated areas (in grey) used for analysis of the deposit height profiles. For a detailed explanation of the analysis methodology followed, see Text S1. The depicted height profile corresponds to a deposit formed after the evaporation of a 0.8 µL drop of a suspension (5 mg/mL) containing silica nanoparticles with 100% SiOH groups on their surface.

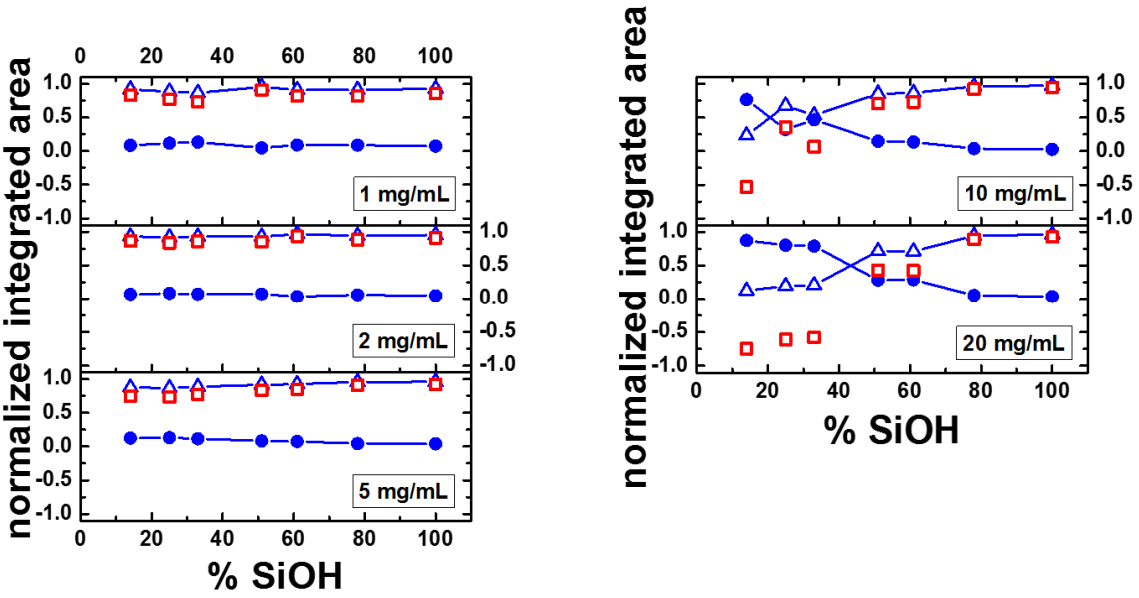

Figure S9. Quantification of dry pattern evolution as a function of particle hydrophobicity for silica nanoparticle dispersions of varying particle concentration. The evolutions of normalized ring area A_{ring} (triangles), interior area A_{inter} (circles) as well as their difference A_{ring} - A_{inter} (squares) *versus* the % of SiOH groups on silica nanoparticle surfaces are shown. These results were obtained by analysing the height profiles shown in Figures 2 and 5.

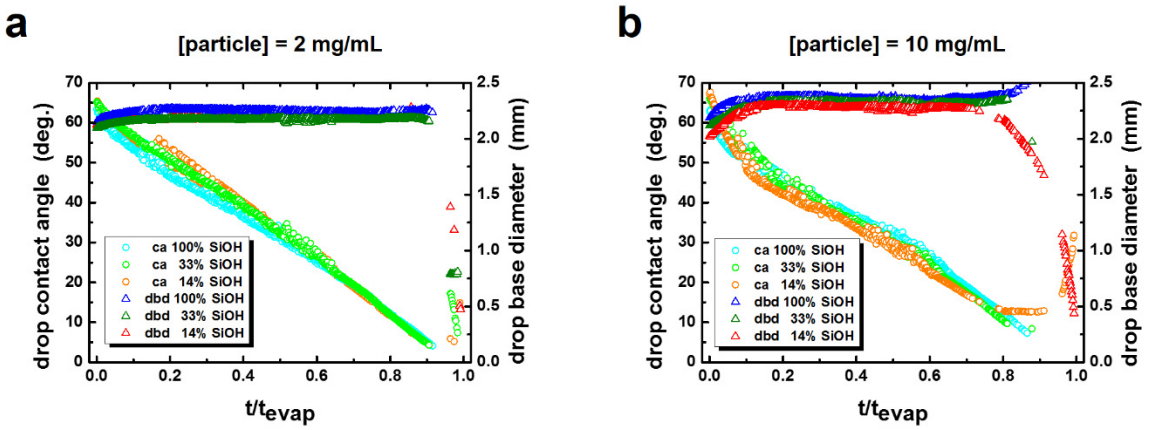

Figure S10. Drop contact angle (ca, circles) and drop base diameter (dbd, triangles) as a function of time (t) normalized by the total evaporation time (t_{evap}) for varying contents of SiOH groups on particle surfaces for particle concentrations of (a) 2 mg/mL and (b) 10 mg/mL. These data were extracted by analyzing Movies S1-S6.

4) Movie Legends

Movie S1. Side-view imaging of the evaporation of a 1.5 μL drop containing 2 mg/mL NPs with 100% SiOH content which was deposited on a glass coverslip. The total evaporation time was approximately 735 s. The temperature and relative humidity were 21.9 ºC and 23 %, respectively. The video is displayed at 30× times the actual speed; the window size is 2.754 mm × 2.065 mm.

Movie S2. Side-view imaging of the evaporation of a 1.5 μL drop containing 2 mg/mL NPs with 33% SiOH content which was deposited on a glass coverslip. The total evaporation time was approximately 618 s. The temperature and relative humidity were 22.2 ± 0.4 ºC and 23 %, respectively. The video is displayed at 30× times the actual speed; the window size is 2.754 mm × 2.065 mm.

Movie S3. Side-view imaging of the evaporation of a 1.5 μL drop containing 2 mg/mL NPs with 14% SiOH content which was deposited on a glass coverslip. The total evaporation time was approximately 590 s. The temperature and relative humidity were 22.4 ± 0.2 ºC and 23 %, respectively. The video is displayed at 30× times the actual speed; the window size is 2.754 mm × 2.065 mm.

Movie S4. Side-view imaging of the evaporation of a 1.5 μL drop containing 10 mg/mL NPs with 100% SiOH content which was deposited on a glass coverslip. The total evaporation time was approximately 659 s. The temperature and relative humidity were 21.9 ºC and 24 %, respectively. The video is displayed at 30× times the actual speed; the window size is 2.810 mm × 2.107 mm.

Movie S5. Side-view imaging of the evaporation of a 1.5 μL drop containing 10 mg/mL NPs with 33% SiOH content which was deposited on a glass coverslip. The total evaporation time was approximately 664 s. The temperature and relative humidity were 21.9 ºC and 24 %, respectively. The video is displayed at 30× times the actual speed; the window size is 2.810 mm × 2.107 mm.

Movie S6. Side-view imaging of the evaporation of a 1.5 μL drop containing 10 mg/mL NPs with 14% SiOH content which was deposited on a glass coverslip. The total evaporation time was approximately 598 s. The temperature and relative humidity were 21.7 ºC and 24 %, respectively. The video is displayed at 30× times the actual speed; the window size is 2.810 mm × 2.107 mm.